Accepted Manuscript online: 2023-01-12 Article published online: 2023-02-13

A Low-Temperature Curable Conformal Adhesive Layer for Monolithic Lamination of Thin Film Encapsulation

Yong Cheon Park[#a]
Kihoon Jeong[#a]
Dahye Ahn[a]
Youson Kim[a]
Sung Gap Im[*a,b]

[a] Department of Chemical & Biomolecular Engineering, Korea Advanced Institute of Science and Technology, 291 Daehak-ro, Yuseong-gu, Daejeon 34141, Republic of Korea
[b] KAIST Institute for NanoCentury, Korea Advanced Institute of Science and Technology, 291 Daehak-ro, Yuseong-gu, Daejeon 34141, Republic of Korea
[*] sgim@kaist.ac.kr
[#] These authors contributed equally to this work.

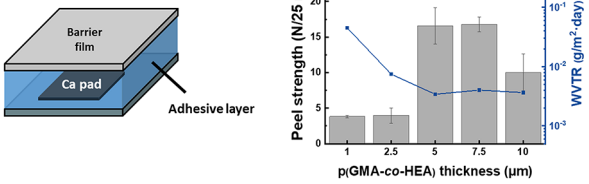

Received: 25. 10. 2022
Accepted after revision: 12.01.2023
DOI: 10.1055/a-2012-2147; Art ID: OM-2022-10-0047-SC

Abstract Lamination of a thin film encapsulation (TFE) layer is regarded as one of the most promising methods that enable the reliable operation of organic electronic devices by attaching the TFE layers thereon directly using an adhesive layer. In this study, a low-temperature curable adhesive thin film with low glass transition temperature (T_g) is newly designed and synthesized. Low T_g allows conformal contact at the interface of the adhesive layer and the substrate subsequently leads to the enhancement of adhesion, and thus the barrier performance of the lamination of barrier film increases. In order to fabricate a low-T_g adhesive layer, glycidyl methacrylate (GMA) was copolymerized with a 2-hydroxyethyl acrylate (HEA) monomer in the vapor phase via initiated chemical vapor deposition. With a 5 μm thick p(GMA-*co*-HEA) adhesive layer, a strong adhesion was readily achieved by curing it at 60 °C for 1 h, with the peel strength of 16.6 N/25 mm, and the water vapor transmission rate of the glass-laminated encapsulation was as low as 3.4×10^{-3} g/m^2·day under accelerating conditions (38 °C, 90% relative humidity). We believe the low-temperature curable thin adhesive layer will serve as a powerful material for the lamination of organic electronic devices in a damage-free way.

Key words: initiated chemical vapor deposition (iCVD), thin film encapsulation (TFE), low-T_g adhesive

Introduction

Organic electronic materials often exhibit outstanding device performance along with its mechanical flexibility, which allows for a wide range of device applications with excellent compatibility with various form factors such as fiber, textile, and patch.[1–5] Although the efficiency of the organic electronic devices increases continuously, the susceptibility to water vapor and oxygen is still one of the biggest hurdles to overcome to achieve the long-term reliable operation thereof.[6,7] Therefore, it is critically important to secure a high-performance encapsulation method to protect the organic electronic devices from the penetration of water vapor and oxygen.[8] Thin film encapsulation (TFE) is one of the most widely investigated encapsulation methods especially in the field of organic light-emitting diode (OLED) displays. TFE consists of an alternating stack of inorganic and organic thin layers directly deposited on the target devices. Generally, the inorganic layer is mainly responsible for blocking the penetration of water vapor and oxygen, and it is essential to fabricate a defect-free inorganic thin film to guarantee the excellent barrier performance. Rather than a single inorganic layer, multiple alternating stacks of inorganic layer with organic layer are well recognized to be much more efficient in terms of the barrier performance to decouple the defects thereof and to provide tortuous penetration path for water vapor and oxygen.[9] However, the repetitive inorganic and organic layer deposition steps are quite tedious and cost-consuming and undesirable damages may also arise from the high-energy deposition process of inorganic layer to the organic electronic devices.

Instead of the complicated fabrication process of TFE and its direct application to OLED displays, a simple encapsulation can be achieved by laminating a pre-produced TFE with an adhesive layer.[10–12] Therefore, the damage to the OLED device can be minimized as far as the lamination process temperature is sufficiently low. Moreover, the method of lamination of TFE is fully compatible with flexible devices when employing a flexible barrier sheet and an adhesive layer with low elastic modulus.[13] With this method, the neutral plane can also be aligned near to the OLED device, which is of central importance to ensure the reliable operation of

flexible OLEDs. To laminate the encapsulation film on the device, a UV-curable adhesive had been utilized widely for the lamination of the barrier film on the target OLEDs.[14,15] Despite the simpleness together with the rapid curability of the UV-curable adhesive, it has been reported that the curing procedure of the UV-curable adhesive may damage perovskite solar cells or other organic electronic devices due to the UV-related damage or the outgassing from the UV-curable adhesive.[10] To avoid this problem, an optically clear adhesive (OCA) with minimized outgassing during the curing process is used widely in the production of OLED-based display products.[16]

However, the thickness of OCA is usually in the order of a few tens of micron, which is quite thick for the applications requiring high-resolution displays or micro-display, which often suffer from light leakage from the side edge of each pixel.[17] Therefore, it is necessary to scale down the thickness of the laminating adhesive layer without compromising the adhesion strength and the damage-free nature of the curing process.

Herein, a copolymer of glycidyl methacrylate (GMA) and 2-hydroxyethyl acrylate (HEA), (p(GMA-*co*-HEA)), is designed as a thermally curable low-temperature adhesive layer, and realized as a thin film via synthesis in the vapor phase (Figure 1a). GMA is a monomer containing a reactive, thermally curable epoxy functionality, whereas the HEA monomer contains a hydroxyl functional group, which can initiate a ring-opening reaction of the epoxide group at low temperature (60 °C). The curing reaction of p(GMA-*co*-HEA) involves only an addition reaction, and thus it does not gen-

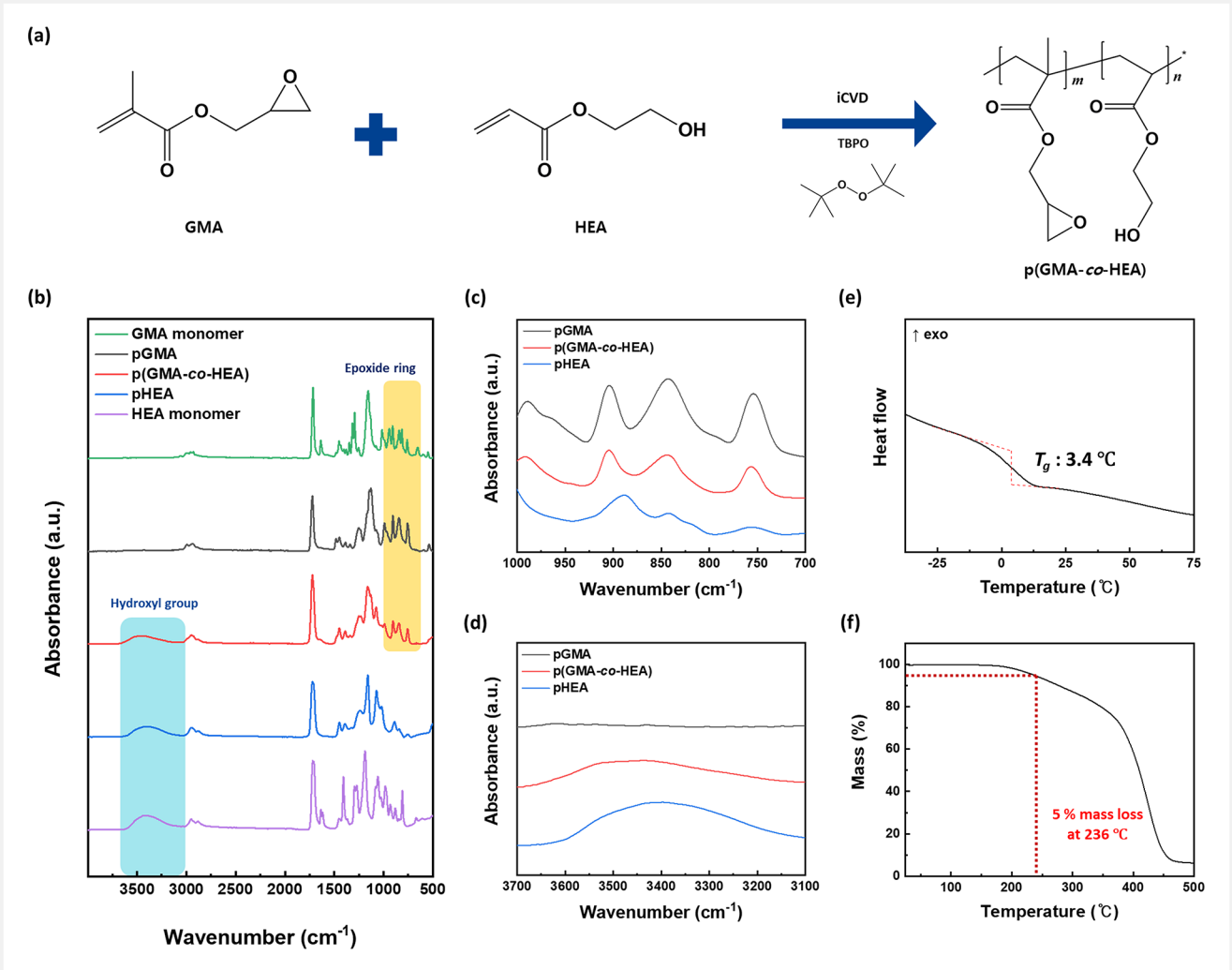

Figure 1 (a) Chemical structures of GMA, HEA, and p(GMA-*co*-HEA) synthesized via the iCVD process. (b) FT-IR spectra of the GMA monomer (green), HEA monomer (purple), pGMA (black), pHEA (blue), and p(GMA-*co*-HEA) (red). Zoomed-in image of the FT-IR spectra of pGMA (black), pHEA (blue), and p(GMA-*co*-HEA) (red) in the range of (c) 1000 – 700 cm^{-1} and (d) 3700 – 3100 cm^{-1}. (e) T_g of p(GMA-*co*-HEA) measured by DSC. (f) TGA of p(GMA-*co*-HEA).

erate any gaseous by-product during the thermal curing process. The copolymer film was synthesized via an initiated chemical vapor deposition (iCVD) process, where the GMA and HEA monomers form a homogeneous mixture in the gas phase, leading to the synthesis of a homogeneous copolymer film of p(GMA-*co*-HEA) conformally on the surface of the target substrate. With only 5 µm thick p(GMA-*co*-HEA) layer, a strong adhesion as well as excellent barrier performance could be achieved.

Results and Discussion

The detailed deposition conditions for pGMA, pHEA, and p(GMA-*co*-HEA) copolymer films are summarized in Table 1. Figure 1b shows Fourier transform infrared (FT-IR) spectra of the GMA monomer, pGMA, HEA monomer, pHEA, and p(GMA-*co*-HEA).[18] The C=C stretch peak of the vinyl bond at 1410 cm^{-1} in the spectra of GMA and HEA monomers disappeared in the spectra of the polymer thin films (pGMA, pHEA, and p(GMA-*co*-HEA)), which confirms that the polymerization was successfully achieved via the iCVD process. In the spectra of pGMA and p(GMA-*co*-HEA), the absorbance peaks at 759, 847, and 907 cm^{-1} associated with the epoxide ring were observed (Figure 1c).[19] The broad peak corresponding to the hydroxyl peak around 3400 cm^{-1} in HEA was detected in the spectra of p(GMA-*co*-HEA) and pHEA as well (Figure 1d). Existence of both the epoxide group from GMA and the hydroxyl group from HEA indicates that copolymerization of GMA and HEA was successfully achieved without the loss of the core functionalities during the polymerization. To check the T_g of p(GMA-*co*-HEA), differential scanning calorimetry (DSC) analysis was performed (Figure 1e).[20] Compared to the T_g of pGMA (55.3 °C) reported in our previous study,[21] the T_g of p(GMA-*co*-HEA) was far lower; 3.4 °C, mainly due to the addition of the soft HEA segment to the copolymer film. The low T_g of p(GMA-*co*-HEA) is highly advantageous in that it can form a good conformal interface with various types of TFE layers and substrate materials. Figure 1f shows thermogravimetric analysis (TGA) data of p(GMA-*co*-HEA). p(GMA-*co*-HEA) exhibited good thermal stability up to 236 °C with only 5% of mass loss.[22]

Table 1 Deposition conditions for pGMA, pHEA, and p(GMA-*co*-HEA)

Polymer	Flow rate (sccm[a])			Pressure (mTorr)	Process temperature (°C)
	GMA[b]	HEA[c]	TBPO[d]		
pGMA	0.492	0	0.439	140	27
p(GMA-*co*-HEA)	0.492	0.391	0.439	140	27
pHEA	0	0.391	0.439	140	27

[a]Standard cc per minute, [b]glycidyl acrylate, [c]2-hydroxyethyl acrylate, and [d]*tert*-butyl peroxide.

Since p(GMA-*co*-HEA) contains an epoxide group, it can be crosslinked readily by applying thermal energy to trigger the thermal curing process. However, active materials in organic electronic devices are susceptible to high temperature, usually greater than 100 °C,[23,24] and the post-curing temperature should be kept lower than 100 °C. The epoxide group can undergo a self-crosslinking reaction, but the onset temperature of the ring-opening reaction from the epoxy ring only is generally too high for organic materials to endure – often greater than 150 °C.[25] Fortunately, the hydroxyl group in HEA expedites the ring-opening reaction of the epoxide ring substantially, which allows low-temperature curing of the copolymer adhesive layer as low as 60 °C. To measure the adhesion strength after curing p(GMA-*co*-HEA), the T-peel test was conducted to polyethylene terephthalate (PET) substrates laminated with each other via a 5-µm-thick p(GMA-*co*-HEA) adhesive layer, as shown in Figure 2a.[26] Figure 2b shows the peel strength of the PET sample laminated at 60 °C with various curing times. Since a longer curing time allows for an increased crosslinking density of p(GMA-*co*-HEA), the peel strength also increases accordingly from 3.53 N/25 mm when cured for 10 min to 6.33 N/25 mm

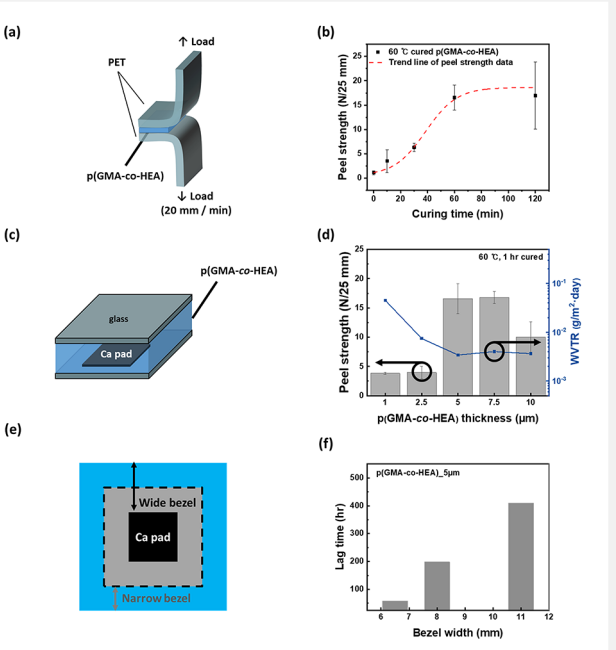

Figure 2 (a) A scheme of peel strength test method. (b) Peel strength of the laminated PET substrates using 5 µm thick p(GMA-*co*-HEA) cured at 60 °C with respect to the curing time. (c) A scheme of Ca test method: Ca film deposited on a glass substrate and laminated with glass lid encapsulation by the 5-µm-thick p(GMA-*co*-HEA) adhesive layer. (d) Peel strength (gray) and WVTR (blue) of the glass substrates laminated using p(GMA-*co*-HEA), followed by curing at 60 °C with respect to the p(GMA-*co*-HEA) layer thickness. (e) An illustration of a Ca test sample with definition of the bezel. (f) Lag time of a glass-laminated Ca test sample with respect to the bezel width.

and 16.6 N/25 mm after 30 min and 60 min of curing, respectively. However, the peel strength of the 120 min-cured sample seems apparently saturated to 17.0 N/25 mm, and we assume 60 min curing is long enough to induce a sufficient amount of crosslinking in the p(GMA-*co*-HEA) adhesive layer.

In order to evaluate the barrier property of the p(GMA-*co*-HEA) adhesive layer, a glass cover was laminated on the Ca-test sample by using a p(GMA-*co*-HEA) adhesive layer as shown in Figure 2c.[27] Since water vapor and oxygen cannot penetrate through the glass, the thickness of the adhesive layer turned out to be a critical factor for both adhesion strength and barrier performance. With a thicker adhesive layer, side penetration of water vapor and oxygen becomes dominant. On the other hand, undesirable particles or surface roughness on the substrate cannot be fully covered tightly by a too thin adhesive layer, resulting in the formation of a void space, which can be another penetration path of water vapor and oxygen. Therefore, it is important to keep the thickness of the adhesive layer as low as possible, while minimizing the formation of void space, which can be accomplished by using an ultrathin adhesive layer capable of forming a conformal contact with the rough substrate surface. The copolymer adhesive layer with low T_g developed in this study can enhance the performance of barrier film lamination.

The peel strength and water vapor transmission rate (WVTR) of the p(GMA-*co*-HEA) adhesive layer with various thicknesses are shown in Figure 2d. A 5-μm-thick p(GMA-*co*-HEA) layer exhibited the highest peel strength of 16.6 N/25 mm, and the lowest WVTR of 3.4×10^{-3} g/m^2·day under the accelerating conditions of 38 °C and 90% relative humidity (RH) was achieved by laminating a glass cover on the Ca test sample. Reducing the thickness of p(GMA-*co*-HEA) to 2.5 μm and 1 μm causes deterioration of both adhesion and barrier properties. On the other hand, the WVTR value seems to be saturated at a higher adhesive thickness, while the peel strength decreased gradually, because the cohesion failure from the soft adhesive layer becomes dominant with a thicker adhesive layer. Compared to other adhesive layers applied for barrier film lamination as shown in Table S1, p(GMA-*co*-HEA) developed in this study with minimized thickness and mild curing conditions can guarantee a reliable operation of electronic devices consisting of various organic materials. Since the side-penetration of water vapor and oxygen significantly affects the barrier property of the laminated encapsulation, barrier property variation along with the size of the bezel width was also analyzed. As shown in Figure 2e, the bezel of the Ca test sample was defined as a width between the Ca pad and the edge of the glass substrate. A wider bezel delays the permeation of water vapor and oxygen, by providing a longer penetration path. Figure 2f shows the lag time calculated from the Ca test sample with various bezel widths. The lag time, which is the time until the Ca pad starts to be oxidized, was only 58.5 h under the accelerating conditions of 38 °C and 90% RH with the bezel of 6.5 mm, but the lag time increased considerably to 198 h and 410 h with the bezel of 8 mm and 11 mm, respectively.

Since the laminated barrier film covers the face side of the organic electronic device, transmittance of the adhesive layer must be maximized for application to optical electronics such as OLEDs or photovoltaics. Figure 3a shows the transmittance of p(GMA-*co*-HEA) in the visible light region (300 – 800 nm).[28] The average transmittance of the 5-μm-thick p(GMA-*co*-HEA) layer was near 100% both before and after curing at 60 °C compared with the glass substrate.

In addition, the compatibility of p(GMA-*co*-HEA) with various barrier films such as a polyethylene naphthalate (PEN) substrate coated with TFE or Al foil was also investigated. To compare the barrier property of barrier film lamination, direct deposition of TFE was performed as shown in Figure 3b with 2.5 dyad TFE consisting of 20 nm thick Al_2O_3 layer/100 nm thick pV3D3 organic layer.[29] Lamination of PEN, a transparent polymer substrate, was covered with 2.5 dyad TFE, to enhance its barrier property, and Al foil, illustrated in Figures 3c and 3d, respectively. Since p(GMA-*co*-HEA) exhibits a low T_g as mentioned above, p(GMA-*co*-HEA) can be deposited to form a conformal contact with various substrate surfaces. Lamination of TFE-deposited PEN and Al foil successfully covered the Ca-deposited glass substrate and the barrier properties of each sample are summarized in Figure 3e. The WVTR of TFE directly deposited on the Ca pad was 7.6×10^{-4} g/m^2·day. After lamination, the WVTR values of PEN coated with TFE and Al foil were 6.5×10^{-3} and 4.9×10^{-3} g/m^2·day, respectively. The WVTR values after lamination of the barrier film were slightly higher than the value from direct deposition of TFE by inserting an organic adhesive layer, but still the WVTR values are quite low. Moreover, a p(GMA-*co*-HEA)-based soft but low-temperature-curable adhesive layer not only enabled the lamination of a rigid glass substrate, but also afforded flexible and even transparent barrier films.

Conclusions

In conclusion, a low-temperature curable thin adhesive layer capable of forming a conformal adhesion interface to various substrates was newly developed. A homogeneous copolymer was synthesized in the vapor phase from two monomers of GMA and HEA, which showed quite low T_g of 3.4 °C. The hydroxyl functional group in HEA initiated a ring-opening reaction of the epoxide functionality at a lower temperature and p(GMA-*co*-HEA) exhibited good adhesion properties when cured at a low temperature, 60 °C, not to damage the organic active materials in organic electronic devices. Laminated encapsulation was successfully demonstrated

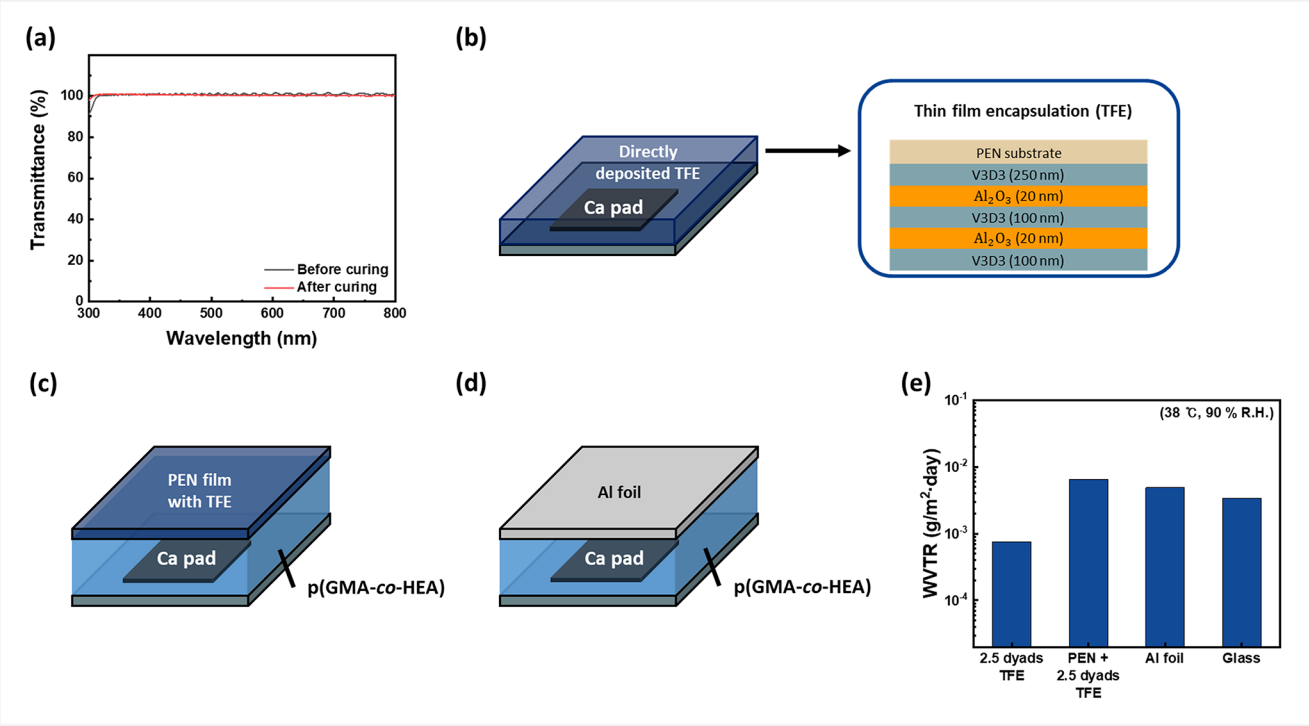

Figure 3 (a) Transmittance of 5 µm thick p(GMA-*co*-HEA) before and after curing at 60 °C for 1 h. (b) Illustration of directly deposited TFE on the Ca test sample and specific structure of 2.5 dyad TFE. Illustration of the Ca test sample laminated with (c) a TFE-deposited PEN film and (d) Al foil. (e) WVTR of directly deposited 2.5 dyad TFE and a Ca test sample laminated with a TFE-deposited PEN film and Al foil.

with a 5-µm-thick p(GMA-*co*-HEA) adhesive layer with the peel strength as high as 16.6 N/25 mm and the WVTR from the glass lamination of 3.4×10^{-3} g/m^2·day. Furthermore, the p(GMA-*co*-HEA) was highly transparent in the whole visible light region and also applicable to lamination of various barrier films with good wettability. This result strongly suggests that the p(GMA-*co*-HEA) layer can enhance the performance of the lamination of the barrier film, which will provide a versatile strategy to ensure reliability and flexibility for the encapsulation methods of the organic electronic devices.

Funding Information

This work was supported in part by the Technology Development Program (S3207541) funded by the Ministry of SMEs and Startups (MSS, Korea) and the Technology Innovation Program (1415181712,RS-2022–00144300) funded by the Ministry of Trade, Industry & Energy (MOTIE, Korea). This work was also supported in part by the Wearable Platform Materials Technology Center (WMC) funded by the National Research Foundation of Korea (NRF) Grant by the Korean Government (MSIT) (NRF-2022R1A5A6000846).

Supporting Information

Supporting Information for this article is available online at https://doi.org/10.1055/a-2012-2147.

Conflict of Interest

The authors declare no conflict of interest.

References and Notes

(1) Jeon, Y.; Noh, I.; Seo, Y. C.; Han, J. H.; Park, Y.; Cho, E. H.; Choi, K. C. *ACS Nano* **2020**, *14*, 15688.
(2) Cho, S. H.; Lee, J.; Lee, M. J.; Kim, H. J.; Lee, S. M.; Choi, K. C. *ACS Appl. Mater. Interfaces* **2019**, *11*, 20864.
(3) Hwang, Y. H.; Kwon, S.; Shin, J. B.; Kim, H.; Son, Y. H.; Lee, H. S.; Noh, B.; Nam, M.; Choi, K. C. *Adv. Funct. Mater.* **2021**, *31*, 2009336.
(4) Choi, S.; Jo, W.; Jeon, Y.; Kwon, S.; Kwon, J. H.; Son, Y. H.; Kim, J.; Park, J. H.; Kim, H.; Lee, H. S.; Nam, M.; Jeong, E. G.; Bin Shin, J.; Kim, T.-S.; Choi, K. C. *npj Flexible Electron.* **2020**, *4*, 33.
(5) Jeon, Y.; Choi, H. R.; Park, K. C.; Choi, K. C. *J. Soc. Inf. Disp.* **2020**, *28*, 324.
(6) Cheng, P.; Zhan, X. *Chem. Soc. Rev.* **2016**, *45*, 2544.

(7) Burrows, P. E.; Bulovic, V.; Forrest, S. R.; Sapochak, L. S.; McCarty, D. M.; Thompson, M. E. *Appl. Phys. Lett.* **1994**, *65*, 2922.
(8) Park, Y. C.; Kim, T.; Shim, H. R.; Choi, Y.; Hong, S.; Yoo, S.; Im, S. G. *Appl. Surf. Sci.* **2022**, *598*, 153874.
(9) Seo, S.-W.; Chae, H.; Joon Seo, S.; Kyoon Chung, H.; Min Cho, S. *Appl. Phys. Lett.* **2013**, *102*, 161908.
(10) Ma, S.; Bai, Y.; Wang, H.; Zai, H.; Wu, J.; Li, L.; Xiang, S.; Liu, N.; Liu, L.; Zhu, C.; Liu, G.; Niu, X.; Chen, H.; Zhou, H.; Li, Y.; Chen, Q. *Adv. Energy Mater.* **2020**, *10*, 1902472.
(11) Seo, H. K.; Park, M. H.; Kim, Y. H.; Kwon, S. J.; Jeong, S. H.; Lee, T. W. *ACS Appl. Mater. Interfaces* **2016**, *8*, 14725.
(12) Park, M. H.; Kim, J. Y.; Han, T. H.; Kim, T. S.; Kim, H.; Lee, T. W. *Adv. Mater.* **2015**, *27*, 4308.
(13) Jo, W.; Lee, H.; Lee, Y.; Bae, B.-S.; Kim, T.-S. *Adv. Eng. Mater.* **2021**, *23*, 2001280.
(14) Han, Y.; Meyer, S.; Dkhissi, Y.; Weber, K.; Pringle, J. M.; Bach, U.; Spiccia, L.; Cheng, Y.-B. *J. Mater. Chem. A* **2015**, *3*, 8139.
(15) Dong, Q.; Liu, F.; Wong, M. K.; Tam, H. W.; Djurisic, A. B.; Ng, A.; Surya, C.; Chan, W. K.; Ng, A. M. *ChemSusChem* **2016**, *9*, 2597.
(16) Park, Y.-T.; Kim, S.; Ham, S. B.; Cho, S. M. *Thin Solid Films* **2020**, *710*, 138277.
(17) Roh, B. G.; Kim, H. I.; Park, S. C.; Baek, J. H.; Park, Y. C.; Kim, Y. *SID Symp. Dig. Tech. Pap.* **2022**, *53*, 776.
(18) Fourier transform-infrared (FT-IR) spectra were measured by using ALPHA FT-IR (Bruker Optics) in absorbance mode, and the measured range of wavenumber was 4000 to 400 cm^{-1} with 4 cm^{-1} resolution.
(19) Kwak, M. J.; Kim, D. H.; You, J. B.; Moon, H.; Joo, M.; Lee, E.; Im, S. G. *Macromolecules* **2018**, *51*, 992.
(20) Thermal analysis of p(GMA-co-HEA) was achieved by differential scanning calorimetry (DSC 214 Polyma, NETZSCH) under N_2 gas conditions and at the heating rate of 10 °C/min.
(21) Jeong, K.; Kwak, M. J.; Kim, Y.; Lee, Y.; Mun, H.; Kim, M. J.; Cho, B. J.; Choi, S. Q.; Im, S. G. *Soft Matter* **2022**, *18*, 6907.
(22) Thermogravimetric analysis was conducted (TG209 F1 Libra, NETZSCH) under N_2 gas conditions and at the heating rate of 10 °C/min.
(23) Han, Y.; Meyer, S.; Dkhissi, Y.; Weber, K.; Pringle, J. M.; Bach, U.; Spiccia, L.; Cheng, Y.-B. *J. Mater. Chem. A* **2015**, *3*, 8139.
(24) Lee, Y. I.; Jeon, N. J.; Kim, B. J.; Shim, H.; Yang, T.-Y.; Seok, S. I.; Seo, J.; Im, S. G. *Adv. Energy Mater.* **2018**, *8*, 1701928.
(25) van de Grampel, R. D.; Ming, W.; van Gennip, W. J. H.; van der Velden, F.; Laven, J.; Niemantsverdriet, J. W.; van der Linde, R. *Polymer* **2005**, *46*, 10531.
(26) Peel strength was measured by T-peel test using universal testing machine (UTM, Zwick) with 5 kN load cell after deposition of p(GMA-*co*-HEA) on a polyethylene terephthalate (PET) film and cured at 60 °C. For the T-peel test, the sample number of $n = 3$ was prepared and the average value with standard deviation of the measured peel strength was calculated.
(27) A Ca test was conducted to calculate the water vapor transmission rate (WVTR). The 50 nm thick Ca (Junsei Chemical, 99.5%) was deposited with the deposition rate of 0.7 Å/s via a thermal evaporator (Daeki Hi-Tech Co., Ltd.) installed in a N_2-filled glove box on the glass substrate. The Ca test samples were stored in a thermohygrostat (JSRH-R70CPL, JS RESEARCH INC.) under the accelerating conditions of 38 °C and 90% RH. After the Ca thin film is oxidized after contact with the water vapor or oxygen, it becomes transparent. Therefore, the barrier property could be monitored in the oxidized area visually. The change of Ca area was analyzed by a digital camera (Nikon P300) and ImageJ v.1.46 (National Institutes of Health). The WVTR could be calculated as: WVTR ($g/m^2 \cdot day$) = $n \cdot \delta_{Ca}\,(M(H_2O))/(M(Ca)) \cdot h \cdot dA/dt$, where n represents the molar equivalent of the Ca oxidation reaction with a water molecule ($n = 2$) and δ_{Ca} is the Ca density (1.55 g/cm^3). Here, $M(H_2O)$ and $M(Ca)$ are the molecular weights of the water molecule and Ca, respectively. h is the height of the Ca film, and dA/dt is the slope of the graph plotting the Ca-oxidized area versus time.
(28) The transmittance of 5 µm thick p(GMA-*co*-HEA) deposited on 1 mm thick glass slide was also obtained by using a spectroscopic ellipsometer (J.A. Woollam Co., Inc.).
(29) For the organic layer and inorganic layer of TFE, poly(1,3,5-trimethyl-1,3,5-trivinylcyclosiloxane) (pV3D3) and Al_2O_3 were deposited, respectively. pV3D3 was deposited via iCVD by using V3D3 (Gelest, 95%) as a monomer and *tert*-butyl peroxide (TBPO, Aldrich, 98%) as an initiator. V3D3 and TBPO were heated to 40 °C and 30 °C, respectively, and fed into a custom-built iCVD system. During the polymer deposition, the process pressure, substrate temperature, and the filament temperature were maintained at 600 mTorr, 50 °C, and 140 °C, respectively. To deposit the Al_2O_3 film via atomic layer deposition (ALD), trimethyl aluminium (TMA, 99.999%, EG Chemical Co. Ltd.) and deionized H_2O were injected sequentially into the ALD chamber. To deposit Al_2O_3 at 90 °C, a single ALD cycle consisted of TMA pulse for 0.5 s, N_2 purging for 15 s, H_2O pulse for 0.5 s, and N_2 purging for 15 s. To accelerate the nucleation step, TMA was injected for 2 s and purged for 30 s in the initial three cycles. The total chamber volume of the reactor was 9210 cm^3, and base pressure was maintained lower than 0.1 Torr.